Published in final edited form as:
*Vis Neurosci*. 2005 ; 22(4): 535–549.

# Stratification of alpha ganglion cells and ON/OFF directionally selective ganglion cells in the rabbit retina

**JIAN ZHANG**[1], **WEI LI**[2], **HIDEO HOSHI**, **STEPHEN L. MILLS**, and **STEPHEN C. MASSEY**
*Department of Ophthalmology and Visual Science, University of Texas Medical School at Houston, Houston*

## Abstract

The correlation between cholinergic sensitivity and the level of stratification for ganglion cells was examined in the rabbit retina. As examples, we have used ON or OFF α ganglion cells and ON/OFF directionally selective (DS) ganglion cells. Nicotine, a cholinergic agonist, depolarized ON/OFF DS ganglion cells and greatly enhanced their firing rates but it had modest excitatory effects on ON or OFF α ganglion cells. As previously reported, we conclude that DS ganglion cells are the most sensitive to cholinergic drugs. Confocal imaging showed that ON/OFF DS ganglion cells ramify precisely at the level of the cholinergic amacrine cell dendrites, and co-fasciculate with the cholinergic matrix of starburst amacrine cells. However, neither ON or OFF α ganglion cells have more than a chance association with the cholinergic matrix. *Z*-axis reconstruction showed that OFF α ganglion cells stratify just below the cholinergic band in sublamina *a* while ON α ganglion cells stratify just below cholinergic *b*. The latter is at the same level as the terminals of calbindin bipolar cells. Thus, the calbindin bipolar cell appears to be a prime candidate to provide the bipolar cell input to ON α ganglion cells in the rabbit retina. We conclude that the precise level of stratification is correlated with the strength of cholinergic input. Alpha ganglion cells receive a weak cholinergic input and they are narrowly stratified just below the cholinergic bands.

### Keywords

Retina; Inner plexiform layer; Confocal microscopy; Alpha ganglion cells; Directional selectivity; ON/OFF DS ganglion cells; Cholinergic amacrine cells; Calbindin bipolar cells

## Introduction

In the mammalian retina, the inner plexiform layer (IPL) is divided into different layers, traditionally numbered 1–5. However, this seems inadequate to describe certain types of narrowly stratified cell and cannot accommodate the large number of cell types now reported. In this paper, we have used confocal microscopy to analyze the stratification level of several ganglion cell types by comparison to the cholinergic bands. Cholinergic amacrine cells are present in all mammalian retinas, including primate (Rodieck & Marshak, 1992), and serve as useful depth markers.

There are 10–12 cone bipolar cell types in the mammalian retina. Each type branches at a characteristic depth in the IPL (Boycott & Wässle, 1991; Hartveit, 1997; Haverkamp et al., 2003; Ghosh et al., 2004; MacNeil et al., 2004) while the rod bipolar cells terminate in

Address correspondence to: Stephen C. Massey, Department of Ophthalmology and Visual Science, University of Texas Medical School at Houston, Houston, TX 77030, USA. E-mail: steve.massey@uth.tmc.edu.
[1]Current address of Jian Zhang: Cullen Eye Institute, Baylor College of Medicine, Houston, TX 77030.
[2]Current address of Wei Li: Department of Ophthalmology, Northwestern Medical School, Chicago, IL 60611.

sublamina 5 (Young & Vaney, 1991; Massey & Mills, 1999). The division of the IPL is functional such that OFF bipolar cells terminate in the upper half, sublamina *a*, while ON bipolar cells, including the rod bipolar cell, terminate in sublamina *b*. Ganglion cells also obey these stratification rules so that OFF ganglion cells branch in sublamina *a*, ON ganglion cells branch in sublamina *b*, and ON/OFF ganglion cells are bistratified with branches in both *a* and *b* (Famiglietti & Kolb, 1976; Bloomfield & Miller, 1986; Amthor et al., 1989*a*,*b*). In the primate retina, there are ON and OFF varieties of both midget and parasol ganglion cells which are stratified at different depths in the IPL (Watanabe & Rodieck, 1989).

Morphological, physiological, and biochemical analyses of ganglion cells all suggest that there are around 12–15 different types (Caldwell & Daw, 1978; DeVries & Baylor, 1997; Marc & Jones, 2002; Rockhill et al., 2002). Each ganglion cell type is thought to carry a separate channel of visual signals but the morphological classification of ganglion cell types has been difficult. Rodieck was among the first to use numerical analyses to classify different ganglion cell types, and he developed an empirical foundation for the idea of a ganglion cell type (Rodieck & Brening, 1983).

Alpha ganglion cells have been described in all mammalian species, including rabbit (Peichl et al., 1987; Peichl, 1991). They have large somas and wide dendritic fields and may be ON or OFF with branches in the appropriate sublayer. Thus, α ganglion cells appear to form a clear example of a neuronal type which recurs across species. ON/OFF DS ganglion cells (Barlow et al., 1964) are bistratified, exactly coincident with the cholinergic bands in the IPL. (Amthor et al., 1984; Famiglietti, 1992; Vaney & Pow, 2000; Dong et al., 2004). They have branches in both sublamina *a* and sublamina *b* and a characteristic retroflexive branching pattern. Morphologically similar types have been reported in other species including primate (Yamada et al., 2005) and mouse (Weng et al., 2005). The depth of stratification in the IPL, which can be accurately visualized by confocal microscopy (Masland & Raviola, 2000), is a primary diagnostic feature to differentiate between different ganglion cell types (Watanabe & Rodieck, 1989).

Cholinergic amacrine cells, also known as starburst amacrine cells due to their unique morphology, form two mirror symmetric populations on either side of the inner plexiform layer (Vaney, 1984; Tauchi & Masland, 1984; Rodieck & Marshak, 1992). The cells in the inner nuclear layer produce OFF responses and stratify in sublamina *a* while the displaced starburst amacrine cells are ON cells branching in sublamina *b*. They are relatively numerous wide-field amacrine cells. Consequently, they have a very high coverage factor and in cross section their dendrites form two continuous bands in the inner plexiform layer which look like train tracks in cross section (Tauchi & Masland, 1985; Famiglietti & Tumosa, 1987). These are very dense, narrowly stratified matrices of overlapping dendrites which cofasciculate with the dendrites of directionally selective ganglion cells (Famiglietti, 1992; Vaney & Pow, 2000; Dong et al., 2004). Starburst amacrine cells are the only source of acetylcholine in the retina but they also contain the inhibitory neurotransmitter gamma aminobutyric acid, GABA (Brecha et al., 1988; Zheng et al., 2004).

In this paper, we have used the above examples of α ganglion cells and ON/OFF DS ganglion cells to determine if the strength of cholinergic input is related to stratification within the cholinergic bands. We have compared the pharmacology of identified ganglion cell types and used confocal microscopy to analyze their depth in the IPL. We show that three specific ganglion cell types are narrowly stratified at distinct depths in the IPL. The ON/OFF DS ganglion cells receive a massive cholinergic input and ramify tightly within the cholinergic bands. In contrast alpha ganglion cells ramify just below the cholinergic bands, do not fasciculate with the cholinergic matrix and receive a limited cholinergic input. Finally,

immunocytochemical markers suggest that the IPL may be divided into as many as 11 separate layers.

## Materials and methods

Adult albino rabbit of both sexes (3–5 kg) were used in these experiments. The retinal preparation was similar to that previously described (Massey & Mills, 1996). In brief, animals were deeply anesthetized with urethane (loading dose 1.5 g/kg, i.p). Following enucleation, the animal was killed by anesthetic overdose and the eye was hemisected. The cornea, lens, and vitreous were removed and the posterior portion of the eye was cut into a few pieces and then immersed in bicarbonate-based Ames' solution (Ames & Nesbett, 1981), which was gassed with 95% $O_2$ and 5% of $CO_2$ at room temperature. Use of animals was approved by the University Committee on Animal Use at the University of Texas, Houston Health Science Center.

### Perfusion

A piece of wholemount retina was placed in a perfusion chamber, and then transferred to a stage mounted on an Olympus BX-50 fixed-stage microscope. The oxygenated Ames' solution flowed by gravity, at a rate of 1–2 ml/min and temperature was maintained at 35°C by a Warner in-line heater (Hamden, CT). Drugs were prepared in 100-fold stock solution and added to Ames' medium in a continuously gassed manifold holding multiple syringe barrels which could be switched to the perfusion line. All drugs were obtained from Sigma (St. Louis, MO), with the exception of NBQX, which was purchased from Tocris Cookson (St. Louis, MO).

### Recording

Sclera attached retinas were used for recording and acridine orange was applied to label cells in the ganglion cell layer in the mid-inferior region. A diffuse light stimulus was generated by a green light-emitting diode (LED) (Nygaard & Frumkes, 1982), which was positioned near the recording chamber and driven sinusoidally by an Axon Digidata 1200 with PClamp software. Sharp intracellular electrodes (200–300 MΩ) were pulled on a Brown-Flaming P-87 horizontal electrode puller (Sutter Instrument, Inc., Novato, CA) and filled with 4% Lucifer Yellow (Molecular Probes, Eugene, OR) in 0.05 mM phosphate buffer (PB) and back filled with 3 M lithium chloride. Cells were viewed through a 40× water immersion lens and once a stable impalement was established with a resting membrane potential more negative than −35 mV, data were recorded and stored on VCR tape (Vetter, Rebersburg, PA) for offline analysis. To visualize the morphology of the cell, the retina was removed from the sclera, placed onto nitrocellulose filter paper, and fixed in 4% paraformaldehyde for 2 h. After washing with phosphate-buffered saline (PBS) containing 0.5% Triton and 0.1% sodium azide, tissue was blocked in 3% donkey serum in PBS/0.5% Triton/0.1% sodium azide for between 3 h and overnight. Then tissue was reacted with antibody against Lucifer yellow (Molecular Probes) for 3–5 days and visualized with donkey anti rabbit/Alexa 488.

### Intracellular dye injection

Isolated pieces of live retina were mounted ganglion cell side-up and labeled with acridine orange as above. ON- or OFF-α ganglion cells and ON–OFF DS ganglion cells were selected by their large soma size and distinctive shape. Following penetration, Lucifer yellow (4%), or Lucifer Yellow, 1%, plus Neurobiotin, 4%, was ejected with 3 Hz negative or biphasic current (1–3 nA) for 4 min. After several cells were dye injected at different locations, the retina was removed from chamber and fixed in 4% paraformaldehyde for 2 h. Cells were stained with the Lucifer Yellow antibody as described above or streptavidin/Alexa 488 and the tissue was subsequently processed for calbindin and choline acetyltransferase (ChAT) immunoreactivity.

### Immunocytochemistry

Immunocytochemistry was conducted followed protocols as previously described (for details see Massey & Mills, 1996). Briefly, wholemount retina or free-floating vibratome sections were blocked with 3% donkey serum in PBS with 0.5% Triton X-100/0.1% sodium azide for 2 h to overnight to reduce nonspecific labeling. Then, the tissues were incubated in a mixture of primary antibodies, usually ChAT (1:100) and calbindin (1:500), in the presence of 1% donkey serum/PBS/with 0.5% Triton X-100/0.1% sodium azide for 5–10 days. Controls that lacked primary antibodies were blank. Following extensive washing with PBS containing 0.5% Triton X-100/0.1% sodium azide, the tissue was incubated overnight with a 1:200 dilution of secondary antibodies conjugated to appropriate fluorochromes, usually Cy-3 and Cy-5 (Jackson Labs, West Grove, PA). After rinsing several times in PBS, the fluorescent specimens were mounted with Vectashield mounting media (Vector, Burlingame, CA) and viewed on a confocal microscope with a krypton-argon laser (Zeiss LSM 410, Zeiss, NY). Images were taken using either 40× or 63× oil objective and processed in Zeiss LSM-PC software. The brightness and contrast of the images were adjusted using Adobe Photoshop.

For quadruple labeling, the retina was incubated in antibodies against protein kinase C (PKC) (rabbit polyclonal, 1:1000, Chemicon, El Segunda, CA), tyrosin hydroxylase (TOH) (rabbit polyclonal, 1:1000, a generous gift from Dr. John Haycock), calbindin (mouse monoclonal, 1:500, Sigma) and ChAT (goat, affinity purified, 1:100, Chemicon). The PKC labeled rod bipolar cells and TOH containing dopaminergic amacrine cells were labeled with the same fluorochrome but these two cell types could be easily distinguished and one was colored magenta using Photoshop.

### Intensity profiles

The profiles across the IPL for each antibody or intracellular stain were obtained using Image Pro to take a histogram along a wide line, essentially averaging the intensity profile. The profiles included the cholinergic bands for reference as depth markers. The line was placed vertically across the IPL, from the inner nuclear layer to the ganglion cell layer. A single line, (i.e. a line width of one pixel) generates a noisy histogram that varies significantly from one region to another. However, if the line width is expanded to include a large section of the IPL, the resulting intensity profile provides an average across the IPL for each fluorescent antibody. The resulting intensity histograms could be downloaded as numerical files and replotted.

### Co-fasciculation analysis

The object was to determine quantitatively how much of a ganglion cell dendritic tree ran within the immunolabeled cholinergic matrix, either in sublamina *a* or *b* as appropriate to the cell type. Photoshop was used to select the dendrites of a dye-injected cell using color and intensity. Within the selected area, green and red pixels were forced to saturation. A 20× objective was used to analyze large portions of the dendritic field and, at this low magnification, cofasciculated dendrites appear to be double labeled, that is, red plus green = yellow. Within the selected dendritic tree, cofasciculation was taken as the number of double-labeled pixels divided by the total pixel number for the selected dendritic tree. The procedure was repeated for the same selected areas after the cholinergic channel had been rotated by 90, 180, or 270 deg to serve as controls.

## Results

### The morphology of α ganglion cells and ON/OFF DS ganglion cells

In material briefly stained with acridine orange, the large somas of alpha ganglion cells and ON/OFF DS ganglion cells were easily recognizable. More detailed morphology was obtained

by filling the cells with Lucifer Yellow and typical examples are shown in Fig. 1. Alpha ganglion cells were large cells with 4 or 5 thick primary dendrites and a rather sparse branching pattern, as described by Peichl et al. (1987). The processes were smooth, running in a radial pattern with branches at relatively acute angles. There were rather few dendritic crossings and large areas with no fine processes between major branches. The dendritic tree was confined to a single focal plane in sublamina *a* for OFF α cells and sublamina *b* for ON α cells.

In contrast, ON/OFF DS ganglion cells were bistratified with a complex space-filling branch pattern. The dendritic tree is highly branched with many fine spines and processes which occasionally appear to form closed loops. The ON and OFF dendritic fields were frequently, but not always, the same size and overlapped roughly, though not exactly. These are the diagnostic properties of ON/OFF DS ganglion cells as first reported by Amthor et al. (1984).

## The pharmacology of α ganglion cells and ON/OFF DS ganglion cells

We wanted to evaluate the strength of the cholinergic input to each ganglion cell type. Therefore, we made intracellular recordings with sharp electrodes from identified cells and perfused the retina with cholinergic agonists or antagonists.

Fig. 2A shows the response of an ON/OFF DS ganglion cell to perfusion with nicotine. The resting membrane potential was −58 mV and a sine-wave driven light stimulus produced ON and OFF responses. At a concentration of (5 $\mu$M), nicotine caused a small depolarization, around 3 mV and a large increase in firing rate, from 12 spikes/s to 46 spikes/s. The same effect was observed in all ON/OFF DS cells ($n$ = 12). This is consistent with earlier results which showed that DS ganglion cells are exquisitely sensitive to cholinergic agonists and 5 $\mu$M is almost a saturating dose for nicotine (Kittila & Massey, 1997).

The responses of an OFF alpha ganglion cell are shown in Fig. 2B. This cell produced a prominent OFF response to diffuse light stimulation. In contrast to the ON/OFF DS cell, when nicotine was applied to an OFF α ganglion cell, the response was much less dramatic with an increase from 14 spikes/s to 18 spikes/s. Nicotine caused only a minor increase in firing rate, even at doses higher than 5 $\mu$M, and the light-driven responses were still evident. As a control, to ensure that the cell was still responsive to external drug application, this cell was also perfused with 10 $\mu$M kainate. As expected, this potent glutamate analog caused a small depolarization and large increase in the firing rate, from 9 spikes/s to 62 spikes/s (Fig. 2B), much greater than the application of nicotinic agonists. The distinct effects of nicotine and kainate were seen in all ON or OFF α ganglion cells ($n$ = 8). Together, these observations indicate that ON/OFF DS ganglion cells are much more sensitive to cholinergic agonists than α ganglion cells.

We also tested the endogenous activation of nicotinic receptors by using hexamethonium, a nicotinic receptor antagonist. As previously reported, hexamethonium (100 $\mu$M) reduced the light-driven response of ON/OFF DS ganglion cells by approximately 50% (Kittila & Massey, 1997). In contrast, hexamethonium did not significantly reduce the number of spikes from ON or OFF α ganglion cells. Similar effects ($n$ = 6) were obtained with tubo-curarine (50 $\mu$M). As above, these results also suggest that ON–OFF DS ganglion cells receive a large nicotinic input compared to α ganglion cells which have a minimal light-driven cholinergic input.

## Ganglion cell stratification

To determine the stratification level in the IPL, ganglion cells were first filled with Lucifer Yellow and then labeled for comparison with well-known markers in the IPL. An antibody against choline acetyltransferase was used to label the two cholinergic bands which we will refer to as cholinergic *a* and cholinergic *b* for the upper (OFF) and lower (ON) bands,

respectively. An antibody against calbindin was used to mark the axons and axon terminals of calbindin bipolar cells, a type of ON cone bipolar cell (Massey & Mills, 1996). The cells were imaged in wholemount and *Z*-axis reconstructions were made along the distal dendrites. The proximal dendrites, close to the soma, were avoided because they are expected to leave the plane of stratification as they descend towards the soma. Images are presented for three ganglion cell types: ON/OFF DS ganglion cells, ON α ganglion cells, and OFF α ganglion cells. The level of stratification was analyzed for at least three cells of each type.

A portion of the dendritic field of an ON α ganglion cell is shown in Fig. 3. In the upper wholemount image, the plane of focus is at the level of the ON α cell dendrites (green) which have a radial pattern and relatively few branches. This is the same level as the calbindin bipolar terminals (blue) which branch at this depth and form a nonrandom mosaic to cover the retina quite evenly. This immediately suggests that the calbindin bipolar terminals are at the right level to provide input to ON α ganglion cells, and it can be seen that there are frequent potential contacts between the ganglion cell dendrites and the bipolar cell axon terminals.

In the triple-label *Z*-axis reconstruction, the axons of the calbindin bipolar cells can be seen descending through the IPL to branch deep in sublamina *b*, below the lower cholinergic band. The cholinergic amacrine cells (red) are located in the inner nuclear layer or displaced to the ganglion cell layer. The processes of the starburst amacrine cells form two bands in the IPL and the ON α ganglion cell is distinctly below cholinergic *b*, the lower cholinergic band, by 2–4 $\mu$m. At this level, the dendrites of the ON α ganglion cell overlap with the terminals of the calbindin bipolar cells. As a result, the ON α dendrite appears cyan in color.

Fig. 4 shows part of the dendritic tree of an ON/OFF DS ganglion cell in wholemount. For clarity, the processes in sublamina *a* are shown in red and those in sublamina *b* are colored green. This cell has the typical highly branched, space-filling dendritic pattern expected for ON/OFF DS ganglion cells. In the *Z*-axis reconstruction, all the ON/OFF DS dendrites are coded green and they can be seen to run exactly within the two cholinergic bands. As a result of the overlap, the ON/OFF DS dendrites appear mostly yellow in the reconstruction. Therefore, the ON/OFF DS ganglion cell is well placed to receive a large cholinergic input to both parts of its bistratified dendritic tree. The calbindin bipolar terminals (blue) are directly below cholinergic *b* and thus could not provide input to either the lower cholinergic band or the ON dendrites of the ON/OFF DS ganglion cell.

Fig. 5 shows the same procedure for an OFF α ganglion cell. In wholemount, the dendritic field has a simple appearance with processes just below the upper cholinergic matrix. As previously reported, OFF α ganglion cells are dye coupled to other α ganglion cells (arrow) and certain wide-field amacrine cells (arrowheads). In the *Z*-axis reconstruction, the stratification level is below cholinergic *a*. Because the OFF α dendrites do not overlap with the other markers, they appear green in the reconstruction, as opposed to yellow or cyan. A small portion of the OFF α dendrite does appear yellow, indicating overlap, but this could be due to a slight ripple in the retina. It is almost impossible to maintain the retina perfectly flat through all stages of manipulation. Thus, the OFF α cell appears to be paramorphic to the ON α cell. The dendrites of α ganglion cells are placed immediately below each cholinergic band with the OFF α dendrites below cholinergic *a* and the ON α cell processes below cholinergic *b*.

The stratification levels for α ganglion cells and ON/OFF DS ganglion cells are summarized in Fig. 6. This figure shows the profile across the IPL for each ganglion cell type for comparison with the position of the cholinergic bands and the calbindin bipolar terminals. The OFF α ganglion cell shows a sharp peak in the IPL, just below cholinergic *a*. The ON/OFF DS ganglion cell is bistratified with two peaks, exactly coincident with the cholinergic bands. The cholinergic band in sublamina *b* is consistently broader than the band in sublamina *a*. The

calbindin profile has two peaks, shown only in the lower two profiles. The major peak, representing the calbindin cone bipolar terminals, is just below cholinergic *b*. A second minor peak, between the cholinergic bands, is due to a calbindin positive wide-field amacrine cell which ramifies in the middle of the IPL. This may mark the approximate position of the *a*/*b* border. Finally, the ON α ganglion cell has a peak coincident with the calbindin bipolar terminals, distinctly below the lower cholinergic band. The width of the ON α cell peak may be particularly narrow because it was derived from one or two dendrites. In comparison, the calbindin bipolar terminals were sampled over a larger area and any minor ripples in the tissue will tend to broaden the peak. In summary, these profiles show that three different ganglion cells stratify at different levels within the IPL, each one specific to its needs.

## Co-fasciculation with the cholinergic matrix

The cholinergic amacrine cells make two dense matrices in the IPL. As previously reported, the ON/OFF DS ganglion cell is co-fasciculated with the dendrites of starburst amacrine cells (Famiglietti, 1992; Vaney & Pow, 2000; Dong et al., 2004). This is shown in Fig. 7, where it can be seen that the dendrites of an ON/OFF DS ganglion cell run almost entirely within the network of cholinergic processes. This is the case, independently, for both the ON and OFF parts of the bistratified tree. In the *Z*-axis reconstruction, the ON/OFF DS ganglion cell dendrites lie within the cholinergic bands.

However, there are two additional factors which can easily confound this apparently simple picture. First, the cholinergic matrices are extremely dense. Thus, any random line drawn across this frame would show a high degree of coincidental overlap with the cholinergic matrix. Second, many of the holes in the cholinergic matrix are filled with the columns of Muller cells which run vertically through the retina. Thus, any process, in trying to avoid the Muller cells, would tend to run with the cholinergic dendrites. To overcome these problems, we quantitatively measured the dendritic length of co-fasciculation for each ganglion cell type and compared the original orientation with versions of the same image where one structure was rotated out of phase by either 90, 180, or 270 deg. As we have shown, the α ganglion cells are stratified at different depths in the retina. However, because the vertical separation from the cholinergic bands is so small, 2–4 $\mu$m, at low magnification, the dendrites of α ganglion cells may also appear to run coincidentally with the cholinergic bundles.

The results of this analysis are shown in Fig. 8. The ON/OFF DS ganglion cell has a high degree of cofasciculation for both parts of the bistratified tree structure. For the ON dendritic tree, 87% of the dendritic length lay within the cholinergic matrix and for the OFF tier, the number was 86%. When one part of the image was rotated, this probability dropped to 48%. Because the two channels of the image were rotated out of phase, this represents chance overlap. For the ON/OFF DS ganglion cell, it is much smaller than the co-fasciculation in the original orientation. In contrast, the ON and OFF α ganglion cells appeared to run in the cholinergic matrix only 51% and 58%, respectively. Most importantly, this was not significantly different for any other orientation. When, one part of the image was rotated out of phase, the degree of overlap was not significantly changed (see also Dong et al., 2004). This indicates that the level of association between α ganglion cells and the cholinergic matrix is merely chance. For the ON/OFF DS cell, the height of the first peak in the original orientation, when compared to the other rotated images, is the signature of true co-fasciculation with the cholinergic matrix. In summary, these results indicate that both tiers of the ON/OFF DS ganglion cell co-fasciculate with the cholinergic network and the α ganglion cells do not.

## Immunolabeling of the inner plexiform layer

Given the limited knowledge of many retina neurons, we set out to label as many structures as possible in vertical sections of the rabbit retina (Fig. 9). Rod bipolar cells were labeled for PKC

(red) and, as expected, their cell bodies were high in the inner nuclear layer (INL) with long thin axons descending through the retina to terminate in large bulbous structures in sublamina 5, at the bottom of the IPL (Young & Vaney, 1991;Massey & Mills, 1999). An antibody against choline acetyltransferase labeled both conventional and displaced amacrine cells as well as two dense bands in the IPL. The calbindin antibody produced strong labeling of laterally extensive horizontal cells in the outer retina and, of more interest here, a population of ON cone bipolar cells (Massey & Mills, 1996). One almost complete calbindin bipolar cell can be seen in the middle of Fig. 9. Its soma lies just beneath the horizontal cells and there is a single axon which descends to sublamina *b* and branches between the rod bipolar terminals and the lower cholinergic band. Finally, an antibody against tyrosine hydroxylase labeled the processes of dopaminergic amacrine cells which run adjacent to the inner nuclear layer in sublamina *a*. In addition, there are a few TOH-positive processes midway between the cholinergic bands. These rather sparse processes could also be dendrites from the dopaminergic amacrine cells or perhaps the type II catecholaminergic amacrine cells (Tauchi et al., 1990). Occasionally, there are processes from calbindin amacrine cells at the midline (Massey & Mills, 1996). Nitric oxide synthase (NOS) positive cells and other wide-field amacrine cells are also known to stratify at this depth (Vaney, 2004).

In the quadruple labeled example shown in Fig. 9, we have numbered potential layers in descending order through the IPL. It should be stressed that these are subjective divisions based on the actual stratification of one of the labeled cell types and the apparent absence of markers in other layers. Layer 1 is marked by the dendrites of dopaminergic amacrine cells immediately adjacent to the amacrine cell layer of the INL. It is well known that the dopaminergic dendrites make rings around AII amacrine cells as they protrude into the IPL (Massey & Mills, 1999). Layer 2 is the empty level between the dopaminergic plexus and cholinergic *a* where several ganglion cells are stratified (Roska & Werblin, 2001). Layer 3 is the upper cholinergic band. The wide unoccupied gap between cholinergic *a* and the midline is designated as layers 4 and 5. The gap is much wider than that occupied by the OFF α ganglion cells in layer 4 and thus seems sufficient to contain at least one more band. Layer 6 is the midline occupied by wide-field amacrine cells and a few dopaminergic processes. It is somewhat scattered in Fig. 9, perhaps because of the presence of descending dendrites which run diagonally until they reach their destination. Two layers, 7 and 8, are assigned to the wide gap between the midline and cholinergic *b*, analogous to layers 4 and 5. Layer 9 is cholinergic *b*. ON α ganglion cells stratify below the lower cholinergic band in layer 10 at the same depth as the axon terminals of calbindin cone bipolar cells. Finally, layer 11 contains the terminals of rod bipolar cells at the bottom of the IPL.

## Discussion

We have examined the morphology and pharmacology of three different types of ganglion cell, the ON α ganglion cell, the OFF α ganglion cell, and the ON/OFF DS ganglion cell. In particular, we report a method to measure the intensity profile across the IPL for each ganglion cell type with reference to the cholinergic bands. Each different ganglion cell branches at a distinct level in the IPL which is correlated with the pharmacological properties of each ganglion cell type. The α ganglion cells, which receive a minor cholinergic input, are narrowly stratified just below the cholinergic bands. These results suggest that depth in the IPL is a simple addressing system and that ganglion cells of a given type are stratified at a specific depth in the IPL.

### Cholinergic input

It is well known that cholinergic drugs affect many or most ganglion cell types (Masland & Ames, 1976; Ariel & Daw, 1982*a*; Baldridge, 1996; Strang et al., 2003) and many ganglion

cell types express nicotinic receptors (Keyser et al., 2000). The effects of cholinergic agonists on most ganglion cell types appear to be direct since they persist during a magnesium or cobalt-induced synaptic blockade (Masland & Ames, 1976; Strang et al., 2003). Ganglion cell types were divided into two groups by Ariel and Daw (1982*a*) who showed that in response to the cholinesterase inhibitor physostigmine, brisk cells had increased spontaneous activity while complex cells had dramatically increased light-driven activity. Of all ganglion cells, the directionally selective subtypes were the most sensitive to physostigmine. Furthermore, nicotine could quickly drive directionally selective ganglion cells into a depolarizing block but other ganglion cell types were never sufficiently excited by nicotine to produce a depolarizing block (Ariel & Daw, 1982*b*).

In the present experiments, we also showed that ON/OFF DS ganglion cells and both ON and OFF α ganglion cells respond to cholinergic agonists. In particular, we found that ON/OFF DS ganglion cells are exquisitely sensitive to nicotine, clearly more so than α ganglion cells. These results are consistent with the effects of hexamethonium, a nicotinic antagonist. As previously reported, hexamethonium completely blocked the action of nicotinic agonists and substantially reduced, but did not eliminate, the light-evoked response of ON/OFF DS ganglion cells (Kittila & Massey, 1997). Thus, a cholinergic input is only part of the excitatory drive to the ON/OFF DS ganglion cell with the remainder supplied by direct input *via* glutamate receptors (Kittila & Massey, 1997). For α ganglion cells, hexamethonium caused a minor reduction in firing rate consistent with a limited or reduced cholinergic input. In summary, these experiments have confirmed previous results that most ganglion cells respond to cholinergic drugs but ON/OFF DS ganglion cells are much more sensitive than α ganglion cells. As we will show below, the division of these ganglion cell types by cholinergic sensitivity is consistent with their depth of stratification in the IPL.

### Co-fasciculation with the cholinergic matrix

Given the sensitivity of the ON/OFF DS ganglion cells to cholinergic drugs, it comes as no surprise that they co-fasciculate with the cholinergic matrix (Famiglietti, 1992; Vaney & Pow, 2000; Dong et al., 2004). The association of ON/OFF DS ganglion cell dendrites with the cholinergic matrix was almost two times higher in the original orientation when compared to a rotated version. This is the signature of true association rather than a random or chance occurrence. Starburst amacrine cells are relatively numerous wide-field cells with a large overlap producing a dense cholinergic matrix, and it has previously been shown that DS ganglion cells co-fasciculate with the dendrites of starburst amacrine cells. In one model of directional selectivity, it was reported that the null side of DS ganglion cells preferentially associated with starburst amacrine cells (Fried et al., 2002), but in a more recent study, the specificity of these connections could not be confirmed (Dong et al., 2004). Both dendritic trees of ON/OFF DS ganglion cells ran within the cholinergic matrix with no apparent preference for the preferred or null directions.

In this paper, we showed that α ganglion cells, a distinct morphological cell type in the rabbit retina, do not co-fasciculate with the cholinergic matrix. While it is true that the dendrites of α ganglion cells often appear, especially at low power, to run with the cholinergic processes, our analysis showed that this did not occur more than for a randomly oriented cell (see also Dong et al., 2004). In other words, the association of α ganglion cell dendrites with the cholinergic matrix does not exceed that of a random line drawn across the field. Casual observation shows that the dendrites of α ganglion cells jump the holes in the cholinergic matrix much more often than the dendrites of ON/OFF DS ganglion cells. The lack of co-fasciculation with the cholinergic matrix is consistent with the relatively low sensitivity of α ganglion cells to cholinergic drugs. It is to be expected if, as we have shown, that both ON and OFF α ganglion cells are stratified outside the cholinergic bands.

### The stratification of α ganglion cells

Our results show rather clearly that α ganglion cells stratify just below the cholinergic bands. This is in close agreement with a classic survey of α ganglion cells in the rabbit retina by Peichl et al. (1987), who described ganglion cells of identical morphology with the OFF α ganglion cell stratified below cholinergic *a* and the ON α ganglion cell stratified below cholinergic *b*. In the cat retina, Vardi et al., (1989) showed an association between α ganglion cells and the cholinergic matrix in the cat retina, but this may reflect a species difference. The ON α ganglion cell is costratified with the terminals of the calbindin bipolar cells, which also ramify 1–3 $\mu$m below cholinergic *b*. Thus, the calbindin bipolar cell appears to be a prime candidate to provide the bipolar cell input to this ganglion cell type in the rabbit retina (Brown et al., 2000).

The α ganglion cells seem identical to the type 11 ganglion cells in the survey reported by Rockhill et al. (2002). However, in this survey, they are drawn as rather broadly stratified, through and beyond the ON/OFF DS or cholinergic bands. This may simply reflect an emphasis on dendritic size and morphology. In fact, depth measurements were made in relation to the borders of the inner nuclear layer and ganglion cell layer and this is inherently less accurate than comparison to a fiducial marker such as the cholinergic bands. Alternatively, the breadth of stratification could indicate the presence of more than one cell type within this classification or possibly variation in the depth of stratification. This latter concept is hard to understand if we expect a given cell type to ramify at a specific depth or address within the IPL. It could be argued that stratification at a different depth, say above instead of below one of the cholinergic bands, would provide different inputs and thus such a ganglion cell would be a different type. We note that another ganglion cell, type 9, in the Rockhill et al. (2002) classification is depicted as branching just above cholinergic *a*.

In a recent analysis, Famiglietti (2004) divides the α-like ganglion cells into seven different types. While we have made no attempt to survey all ganglion cell types, it seems most likely that the α ganglion cells described here correspond to types Ia2 and Ib2, which are noted as a paramorphic pair (Famiglietti, 2004). Type Ia2 is stratified below cholinergic *a* and type Ib2 is stratified below cholinergic *b*, in agreement with the results presented here. Ganglion cells selected for dye filling in this study were those with the largest somas, mostly from peripheral retina, and Ia2 had the largest somas of all ganglion cell types, especially in the periphery (Famiglietti, 2004; see also Marc & Jones, 2002).

In our hands, OFF α ganglion cells were often dye coupled to amacrine cells and other OFF α cells as also reported for type Ia2 ganglion cells (Famiglietti, 2004). OFF α ganglion cells, but not ON α ganglion cells, have been reported as coupled and Hu and Bloomfield (2003) showed that coupling is responsible for synchronous firing among cells of this type. Physiological evidence for synchrony, and therefore coupling, was also found for OFF α but not ON α ganglion cells (DeVries, 1999). It may seem surprising for a paramorphic pair that OFF α cells should be coupled while ON α cells are not. Coupling is labile and some false negatives (i.e. the absence of coupling) could be produced by electrode damage. However, in a biochemical analysis of ganglion cells in the rabbit retina, OFF α ganglion cells (class 9, largest soma size) were consistently found to contain GABA, thought to enter *via* gap junctions with coupled GABA amacrine cells (Marc & Jones, 2002). ON α ganglion cells (class 1a) have a distinct and significantly different signature (Marc & Jones, 2002). This is strong evidence, independent of electrode penetration, that OFF α cells are coupled while ON α cells are not.

Roska and Werblin (2001) also conducted a physiological/morphological survey of rabbit ganglion cells. Among the concentric types, they identified ten different types including several brisk types which could be equivalent to α ganglion cells. A brisk transient OFF cell was located just below cholinergic *a* which is consistent with the results presented here. However, it was not reported as dye coupled. Two ON brisk transient cells were found above cholinergic *b*,

close to the midline, which is not in agreement with the present results. The level of stratification was reported relative to the bistratified ON/OFF DS ganglion cell but the position of these cells seems displaced toward the inner nuclear layer compared to the measurements of others who usually place the cholinergic bands at 20% and 70% (Famiglietti & Tumosa, 1987). Unfortunately, it was not possible to obtain enough detail from the small figures of this preliminary report to compare with the present results.

The general agreement between the above reports is satisfying given the traditional difficulties associated with morphological classifications. Fortunately, α ganglion cells are one of the most recognizable ganglion cell types across mammalian species. Some difficulty still lies in comparing morphological and physiological classifications at different eccentricities, further complicated by cross-species comparisons (Rodieck & Brening, 1983). Perhaps these problems will be resolved as more reliable markers for individual cell types become available and we learn more about distinct ganglion cell types such as the melanopsin ganglion cell (Berson, 2003). The small details, concerning either a difference in depth of a few microns or subtle variations in branch pattern among ganglion cell types, seem to be important. Our results strongly suggest that a specific ganglion cell type is stratified at a precise depth in the IPL and this confirms the work of others who have studied different ganglion cell types (Roska & Werblin, 2001; Rockhill et al., 2002; Famiglietti, 2004).

## Stratification of the IPL

The analysis of the quadruple labeled vertical section in Fig. 9 suggests that the IPL may be divided into 11 layers. This division is somewhat subjective but it is a clear demonstration of the different layers and it places a lower limit on the total number of possible layers. The IPL may be divided into sublamina *a* and *b* which reflect the functional division of OFF and ON layers, respectively. More traditionally, the IPL is divided into 5 sublayers each of which have been further divided into three yielding a total of 15. The true number is unknown. It may reflect the number of bipolar cell inputs or, alternatively, it may reflect the number of ganglion cell outputs. Haverkamp et al. (2003) suggested that the primate IPL is thick enough to accommodate 20 sublayers. The number of cone bipolar cell types in the mammalian retina is usually given between 10 and 12, plus one for the rod bipolar cells (Haverkamp et al., 2003;Ghosh et al., 2004;MacNeil et al., 2004), and there is strong evidence that different bipolar cell types have different physiological properties, thus splitting the photoreceptor signals into different channels (DeVries, 2000). The number of ganglion cell types has been estimated as 13 or 14, but there is usually an unclassified remainder which could include a number of sparse or low-density cell types (Rockhill et al., 2002;Marc & Jones, 2002;Dacey et al., 2003;Yamada et al., 2005). This may boost the total number of types to between 15 and 20. For example, the melanopsin ganglion cell is a distinct type which only accounts for a small fraction, 0.2%, of primate ganglion cells (Dacey et al., 2005). If an assumption is made that each ganglion cell type represents an independent channel in the visual system, this may reflect the total number of layers in the IPL. Some broadly stratified ganglion cells may traverse several layers to gather input from multiple bipolar cells (Brown et al., 2000). Alternatively, some sparse populations could be stratified at the same depth. Nevertheless, the similarity between the number of bipolar cells, the number of ganglion cells and the number of visible layers suggests a functional principle at work.

#### Acknowledgements

This work was supported by NIH Grants EY06515, EY10121, Vision Core Grant EY10608 and Research to Prevent Blindness.

## References


Ames A III, Nesbett FB. *In vitro* retina as an experimental model of the central nervous system. Journal of Neurochemistry 1981;37:867–877. [PubMed: 7320727]

Amthor FR, Oyster CW, Takahashi ES. Morphology of on-off direction-selective ganglion cells in the rabbit retina. Brain Research 1984;298:187–90. [PubMed: 6722555]

Amthor FR, Takahashi ES, Oyster CW. Morphologies of rabbit retinal ganglion cells with concentric receptive fields. Journal of Comparative Neurology 1989a;280:72–96. [PubMed: 2918097]

Amthor FR, Takahashi ES, Oyster CW. Morphologies of rabbit retinal ganglion cells with complex receptive fields. Journal of Comparative Neurology 1989b;280:97–121. [PubMed: 2918098]

Ariel M, Daw NW. Effects of cholinergic drugs on receptive field properties of rabbit retinal ganglion cells. Journal of Physiology (London) 1982a;324:135–160. [PubMed: 7097593]

Ariel M, Daw NW. Pharmacological analysis of directionally sensitive rabbit retinal ganglion cells. Journal of Physiology (London) 1982b;324:161–185. [PubMed: 7097594]

Baldridge WH. Optical recordings of the effects of cholinergic ligands on neurons in the ganglion cell layer of mammalian retina. Journal of Neuroscience 1996;16:5060–5072. [PubMed: 8756436]

Barlow HB, Hill RM, Levick WR. Retinal ganglion cells responding selectively to direction and speed of image motion in the rabbit. Journal of Physiology (London) 1964;173:377–407. [PubMed: 14220259]

Berson DM. Strange vision: Ganglion cells as circadian photoreceptors. Trends in Neuroscience 2003;26:314–320.

Bloomfield SA, Miller RF. A functional organization of ON and OFF pathways in the rabbit retina. Journal of Neuroscience 1986;6:1–13. [PubMed: 3944611]

Boycott BB, Wässle H. Morphological classification of bipolar cells of the primate retina. European Journal of Neuroscience 1991;3:1069–1088. [PubMed: 12106238]

Brecha N, Johnson D, Peichl L, Wässle H. Cholinergic amacrine cells of the rabbit retina contain glutamate decarboxylase and gamma-aminobutyrate immunoreactivity. Proceedings of the National Academy of Sciences of the USA 1988;85:6187–6191. [PubMed: 3413087]

Brown SP, He S, Masland RH. Receptive field microstructure and dendritic geometry of retinal ganglion cells. Neuron 2000;27:371–383. [PubMed: 10985356]

Caldwell JH, Daw NW. New properties of rabbit retinal ganglion cells. Journal of Physiology (London) 1978;276:257–276. [PubMed: 650447]

Dacey DM, Liao HW, Peterson BB, Robinson FR, Smith VC, Pokorny J, Yau KW, Gamlin PD. Melanopsin-expressing ganglion cells in primate retina signal colour and irradiance and project to the LGN. Nature 2005;433:749–754. [PubMed: 15716953]

Dacey DM, Peterson BB, Robinson FR, Gamlin PD. Fireworks in the primate retina: *In vitro* photodynamics reveals diverse LGN-projecting ganglion cell types. Neuron 2003;37:15–27. [PubMed: 12526769]

DeVries SH. Correlated firing in rabbit retinal ganglion cells. Journal of Neurophysiology 1999;81:908–920. [PubMed: 10036288]

DeVries SH. Bipolar cells use kainate and AMPA receptors to filter visual information into separate channels. Neuron 2000;28:847–856. [PubMed: 11163271]

DeVries SH, Baylor DA. Mosaic arrangement of ganglion cell receptive fields in rabbit retina. Journal of Neurophysiology 1997;78:2048–2060. [PubMed: 9325372]

Dong W, Sun W, Zhang Y, Chen X, He S. Dendritic relationship between starburst amacrine cells and direction-selective ganglion cells in the rabbit retina. Journal of Physiology 2004;556:11–17. [PubMed: 14978206]

Famiglietti EV. Dendritic co-stratification of ON and ON-OFF directionally selective ganglion cells with starburst amacrine cells in rabbit retina. Journal of Comparative Neurology 1992;324:322–335. [PubMed: 1383291]

Famiglietti EV. Class I and class II ganglion cells of rabbit retina: A structural basis for X and Y (brisk) cells. Journal of Comparative Neurology 2004;478:323–46. [PubMed: 15384072]

Famiglietti EV Jr, Kolb H. Structural basis for ON-and OFF-center responses in retinal ganglion cells. Science 1976;194:193–195. [PubMed: 959847]

Famiglietti EV Jr, Tumosa N. Immunocytochemical staining of cholinergic amacrine cells in rabbit retina. Brain Research 1987;413:398–403. [PubMed: 3300857]

Fried SI, Munch TA, Werblin FS. Mechanisms and circuitry underlying directional selectivity in the retina. Nature 2002;420:411–414. [PubMed: 12459782]

Ghosh KK, Bujan S, Haverkamp S, Feigenspan A, Wassle H. Types of bipolar cells in the mouse retina. Journal of Comparative Neurology 2004;469:70–82. [PubMed: 14689473]

Hartveit E. Functional organization of cone bipolar cells in the rat retina. Journal of Neurophysiology 1997;77:1716–1730. [PubMed: 9114231]

Haverkamp S, Haeseleer F, Hendrickson A. A comparison of imunocytochemical markers to identify bipolar cell types in human and monkey retina. Visual Neuroscience 2003;20:589–600. [PubMed: 15088712]

Hu EH, Bloomfield SA. Gap junctional coupling underlies the short-latency spike synchrony of retinal αganglion cells. Journal of Neuroscience 2003;23:6768–6777. [PubMed: 12890770]

Keyser KT, MacNeil MA, Dmitrieva N, Wang F, Masland RH, Lindstrom JM. Amacrine, ganglion, and displaced amacrine cells in the rabbit retina express nicotinic acetylcholine receptors. Vis Neuroscience 2000;17:743–52.

Kittila CA, Massey SC. Pharmacology of directionally selective ganglion cells in the rabbit retina. Journal of Neurophysiology 1997;77:675–689. [PubMed: 9065840]

MacNeil MA, Heussy JK, Dacheux RF, Raviola E, Masland RH. The population of bipolar cells in the rabbit retina. Journal of Comparative Neurology 2004;472:73–86. [PubMed: 15024753]

Marc RE, Jones BW. Molecular phenotyping of retinal ganglion cells. Journal of Neuroscience 2002;22:413–427. [PubMed: 11784786]

Masland RH, Ames AI II. Responses to acetylcholine of ganglion cells in an isolated mammalian retina. Journal of Neurophysiology 1976;39:1220–1235. [PubMed: 993829]

Masland RH, Raviola E. Confronting complexity: Strategies for understanding the microcircuitry of the retina. Annual Review of Neuroscience 2000;23:249–284.

Massey SC, Mills SL. A calbindin-immunoreactive cone bipolar cell type in the rabbit retina. Journal of Comparative Neurology 1996;366:15–33. [PubMed: 8866843]

Massey SC, Mills SL. An antibody to calretinin stains AII amacrine cells in the rabbit retina: Double-label and confocal analyses. Journal of Comparative Neurology 1999;411:3–18. [PubMed: 10404104]

Nygaard RW, Frumkes TE. LEDs: Convenient, inexpensive sources for visual experimentation. Vision Research 1982;22:435–440. [PubMed: 7112942]

Peichl L. Alpha ganglion cells in mammalian retinae: common properties, species differences, and some comments on other ganglion cells. Visual Neuroscience 1991;7:155–169. [PubMed: 1931799]

Peichl L, Buhl EH, Boycott BB. Alpha ganglion cells in the rabbit retina. Journal of Comparative Neurology 1987;263:25–41. [PubMed: 2444630]

Rockhill RL, Daly FJ, MacNeil MA, Brown SP, Masland RH. The diversity of ganglion cells in a mammalian retina. Journal of Neuroscience 2002;22:3831–3843. [PubMed: 11978858]

Rodieck RW, Brening RK. Retinal ganglion cells: Properties, types, genera, pathways and trans-species comparisons. Brain, Behavior, and Evolution 1983;23:121–164.

Rodieck RW, Marshak DW. Spatial density and distribution of choline acetyltransferase immunoreactive cells in human, macaque, and baboon retinas. Journal of Comparative Neurology 1992;321:46–64. [PubMed: 1613139]

Roska B, Werblin F. Vertical interactions across ten parallel, stacked representations in the mammalian retina. Nature 2001;410:583–587. [PubMed: 11279496]

Strang CE, Amthor FR, Keyser KT. Rabbit retinal ganglion cell responses to nicotine can be mediated by beta2-containing nicotinic acetylcholine receptors. Visual Neuroscience 2003;20:651–662. [PubMed: 15088718]

Tauchi M, Madigan NK, Masland RH. Shapes and distributions of the catecholamine-accumulating neurons in the rabbit retina. Journal of Comparative Neurology 1990;293:178–189.

Tauchi M, Masland RH. The shape and arrangement of the cholinergic neurons in the rabbit retina. Proceedings of the Royal Society B (London) 1984;223:101–19.

Tauchi M, Masland RH. Local order among the dendrites of an amacrine cell population. Journal of Neuroscience 1985;5:2494–2501. [PubMed: 4032008]

Vaney DI. 'Coronate' amacrine cells in the rabbit retina have the 'starburst' dendritic morphology. Proceedings of the Royal Society B (London) 1984;220:501–508.

Vaney DI. Type 1 nitrergic (ND1) cells of the rabbit retina: comparison with other axon-bearing amacrine cells. Journal of Comparative Neurology 2004;474(1):149–171. [PubMed: 15156584]

Vaney DI, Pow DV. The dendritic architecture of the cholinergic plexus in the rabbit retina: Selective labeling by glycine accumulation in the presence of sarcosine. Journal of Comparative Neurology 2000;421:1–13. [PubMed: 10813769]

Vardi N, Massarachia PJ, Sterling P. Structure of the starburst amacrine network in the cat retina and its association with alpha ganglion cells. Journal of Comparative Neurology 1989;288:601–611. [PubMed: 2808752]

Watanabe M, Rodieck RW. Parasol and midget ganglion cells of the primate retina. Journal of Comparative Neurology 1989;289:434–454. [PubMed: 2808778]

Weng S, Sun W, He S. Identification of ON–OFF direction-selective ganglion cells in the mouse retina. Journal of Physiology 2005;562:915–923. [PubMed: 15564281]

Yamada ES, Bordt AS, Marshak DW. Wide-field ganglion cells in macaque retinas. Visual Neuroscience 2005;22:379–389. [PubMed: 16212696]

Young HM, Vaney DI. Rod-signal interneurons in the rabbit retina: 1. Rod bipolar cells. Journal of Comparative Neurology 1991;310:139–153. [PubMed: 1720140]

Zheng JJ, Lee S, Zhou ZJ. A developmental switch in the excitability and function of the starburst network in the mammalian retina. Neuron 2004;44:851–864. [PubMed: 15572115]

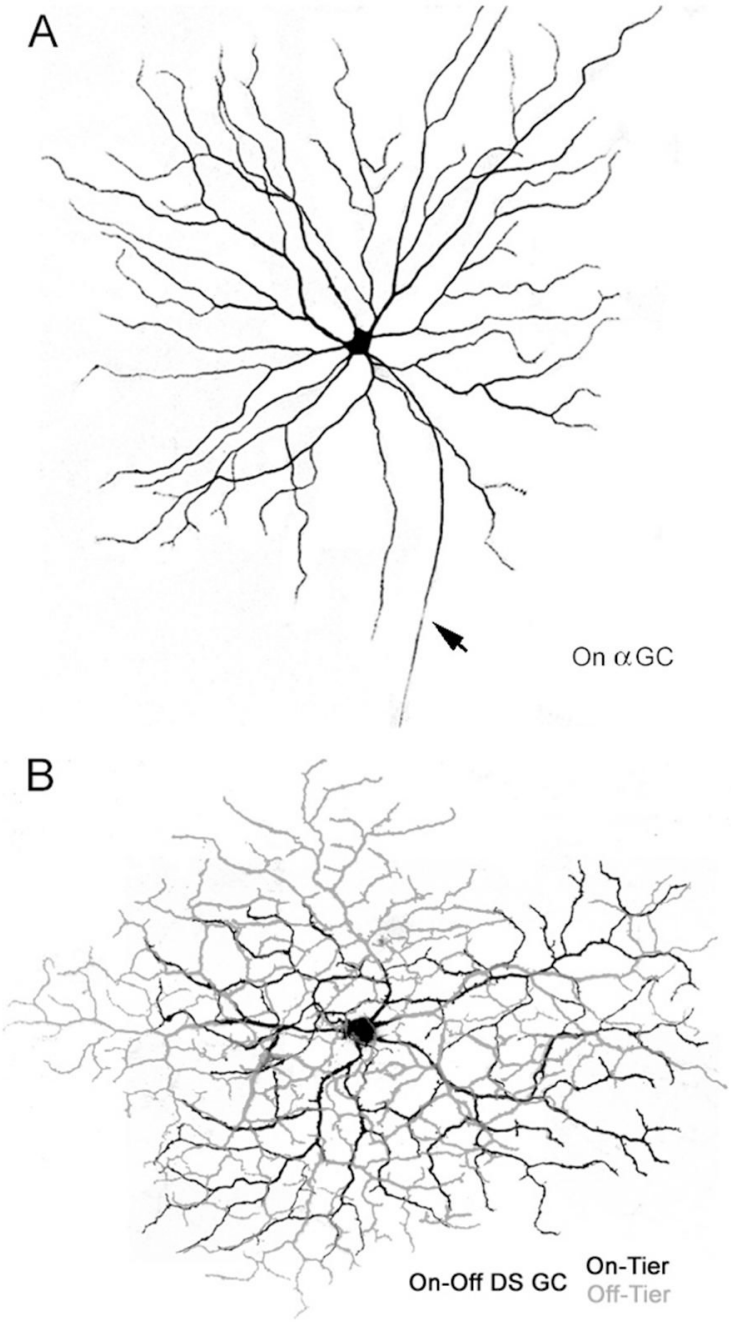


**Fig. 1.**

Montage derived from multiple confocal images of Lucifer yellow-filled ganglion cells. A: An ON α ganglion cell located in mid-inferior retina. This cell has the typical radiate dendritic field with relatively few branch points. Arrow indicates the axon. B: A bistratified ON/OFF DS ganglion cell from mid-inferior retina. The ON dendritic field is shown in black, the OFF dendritic field in gray. They overlap approximately but not exactly. The dendrites make many retroflexive branches. This is the classic appearance of an ON/OFF DS ganglion cell as described by Amthor et al. (1984).

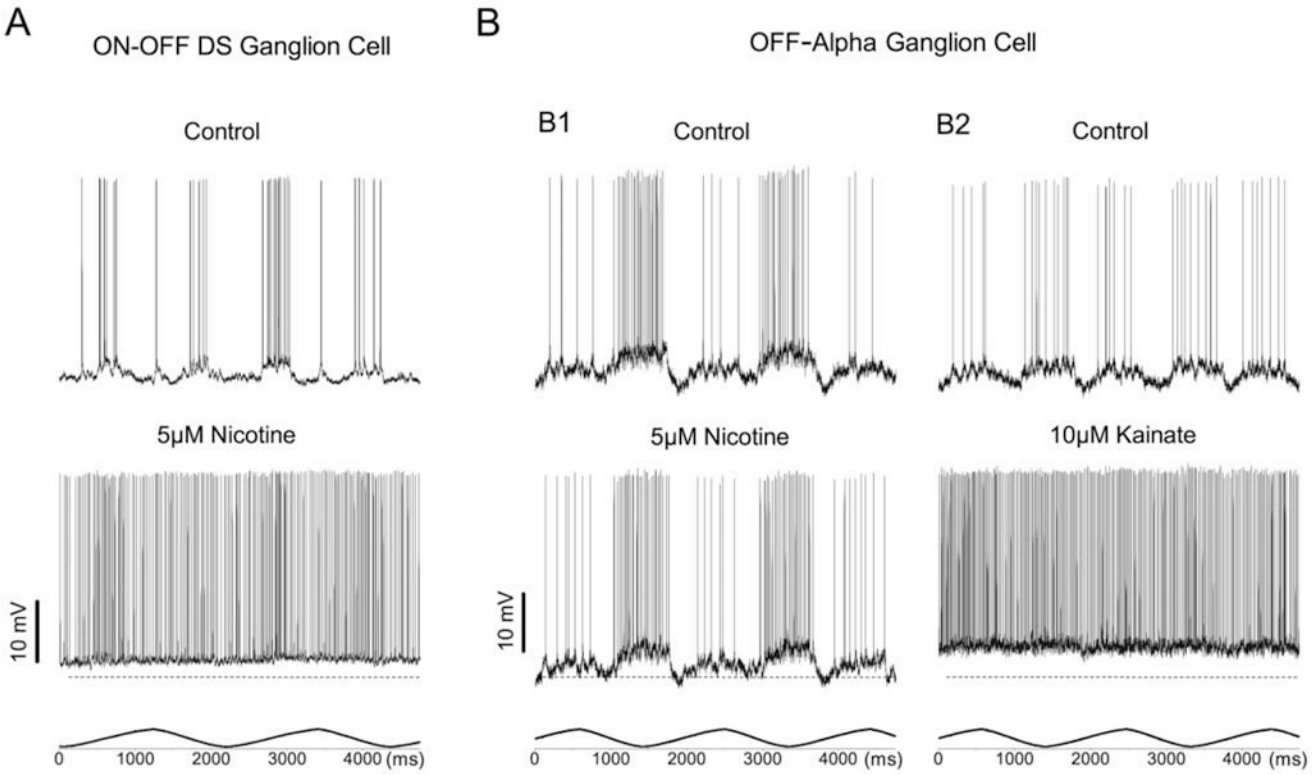


**Fig. 2.**

The effect of nicotine on different ganglion cell types. A: Effect of nicotine on the light response of an ON/OFF DS ganglion cell. *Top:* Control, a sine-wave-driven light stimulus generated an ON and OFF response. *Bottom:* 5 $\mu$M nicotine produced a slight depolarization from the control membrane potential shown by the dotted line and there was a dramatic increase in spike activity. B: Effect of nicotine and kainate on the light response of an OFF α ganglion cell. B1. *Top:* Control, a sine-wave driven-light stimulus produced a strong OFF response. *Bottom:* Nicotine had little effect on the membrane potential and very modest effect on the firing rate. B2: *Top:* Same cell as in B1, after washing out the nicotine, control responses were obtained again. *Bottom:* kainate caused a small depolarization and greatly increased the cell's firing rate. For α ganglion cells, the response to kainate was dramatically stronger than the response to nicotine.

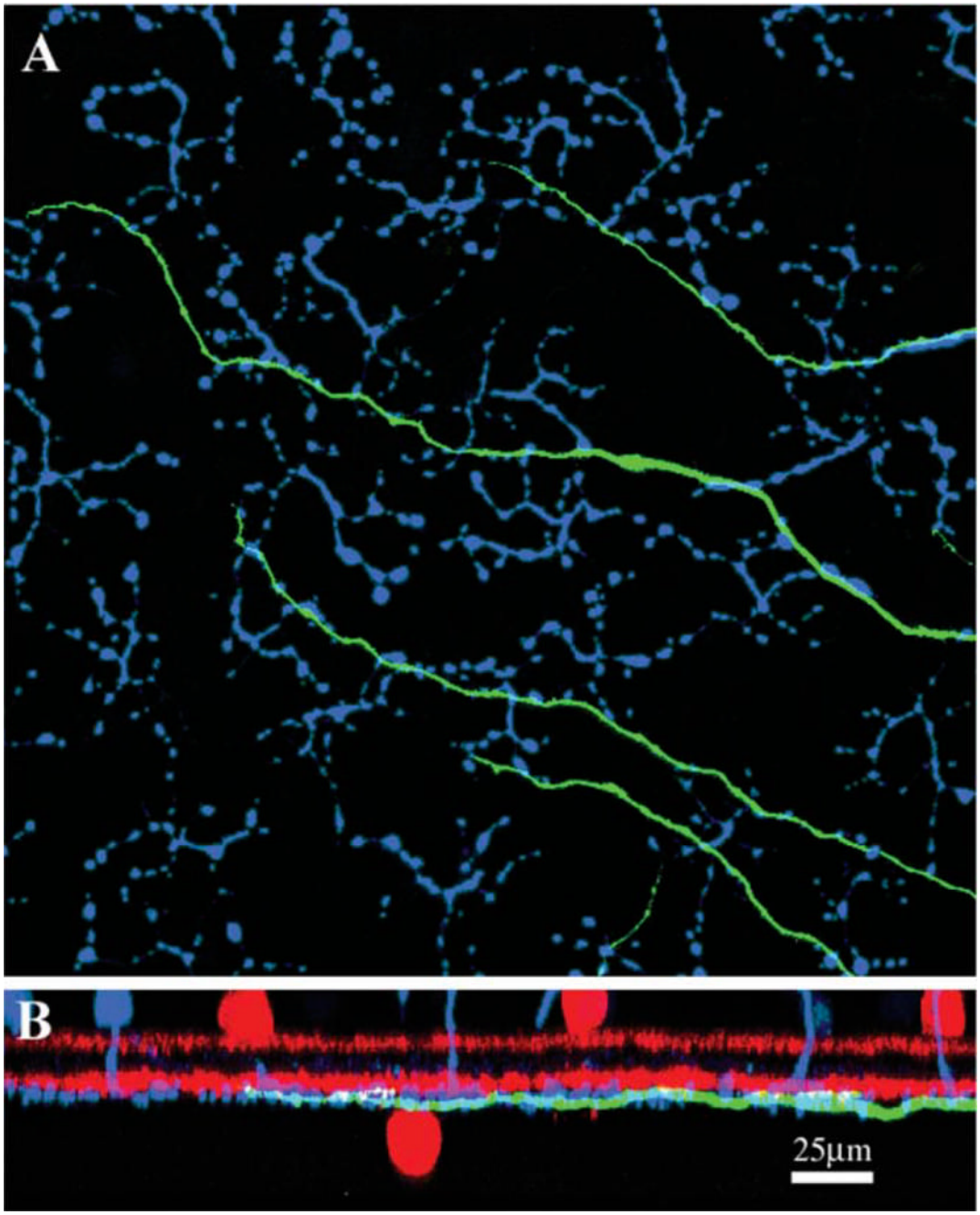


**Fig. 3.**

Triple label confocal images of an ON α ganglion cell. A: Wholemount view of the partial dendritic field of an ON α ganglion cell (green). The axon terminals of calbindin bipolar cells (blue) are found at the same level. Furthermore, there are many close appositions between the ON α cell and the calbindin bipolar terminals which are sites of potential input. The calbindin bipolar cell is the leading candidate to provide excitatory input to ON α ganglion cells in the rabbit retina. B: *Z*-axis reconstruction. Labeling with an antibody against choline acetyltransferase (red) marks conventional and displaced somas of cholinergic amacrine cells and two dense bands at approximately 20% and 70% depth in the IPL. Cholinergic *b* is slightly denser than the upper band. The calbindin bipolar cells (blue) have somas high in the INL and

their axons descend just below cholinergic *b* to from a band of terminals. The dendrites of the ON α ganglion cell (green) lie just below cholinergic *b* at the same level as the terminals of calbindin bipolar cells. Because the ON α cell dendrites are superimposed on the calbindin bipolar terminals, they appear cyan.

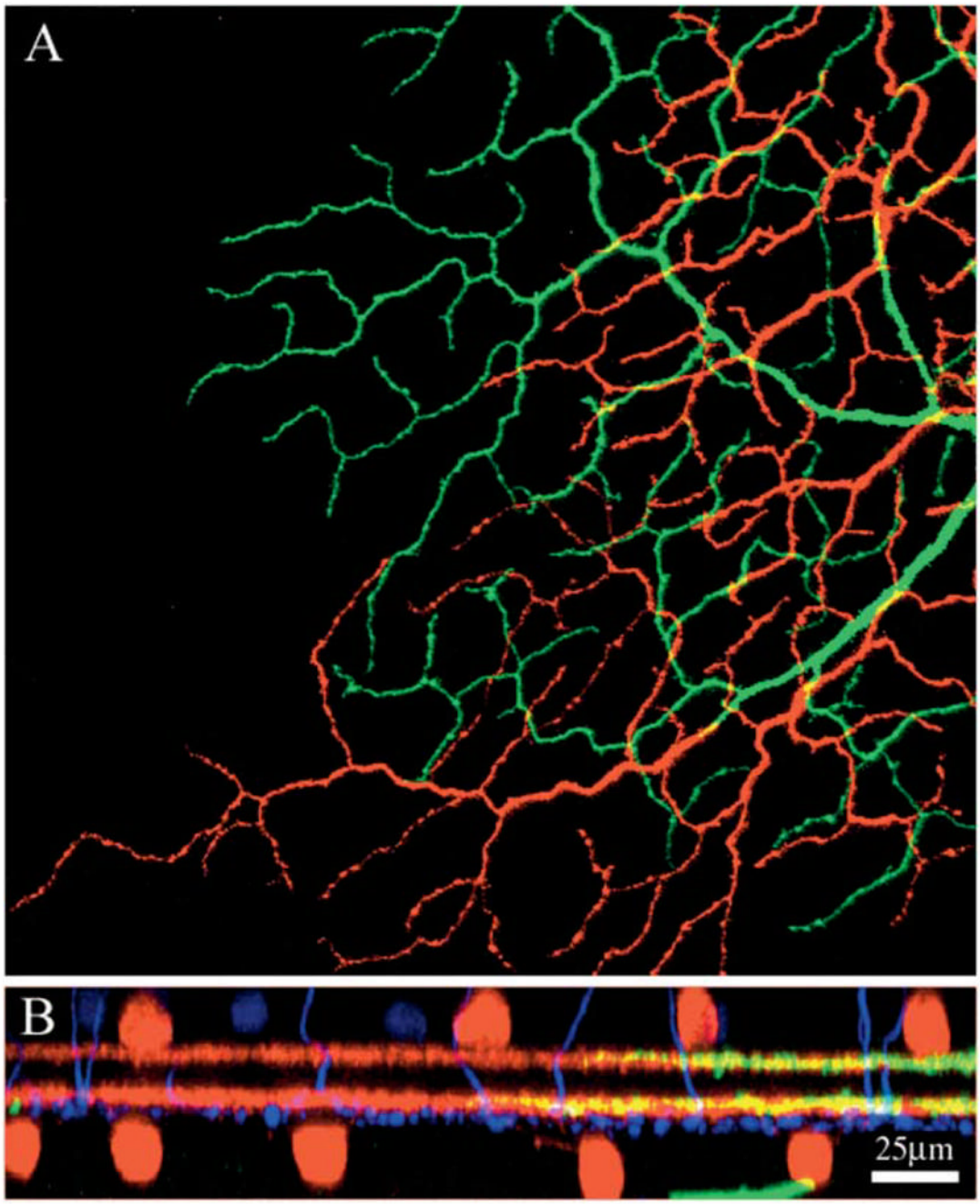


**Fig. 4.**

Triple label confocal images of a bistratified ON/OFF DS ganglion cell A: Wholemount view of a dye-injected ON/OFF DS cell with the OFF dendritic field in red and ON dendritic field in green. B: *Z*-axis reconstruction, cholinergic amacrine cells with two bands in the IPL are shown red. Note the change in color from panel A. Calbindin bipolar cells (blue) descend to just below cholinergic *b*. Dendrites of the bistratified ON/OFF DS cell (green) run exactly in the cholinergic bands. Both ON and OFF dendrites are shown in green. Because, the ganglion cell dendrites are superimposed on the cholinergic matrices, they appear yellow. A piece of the ON/OFF DS cell axon was captured in the ganglion cell layer.

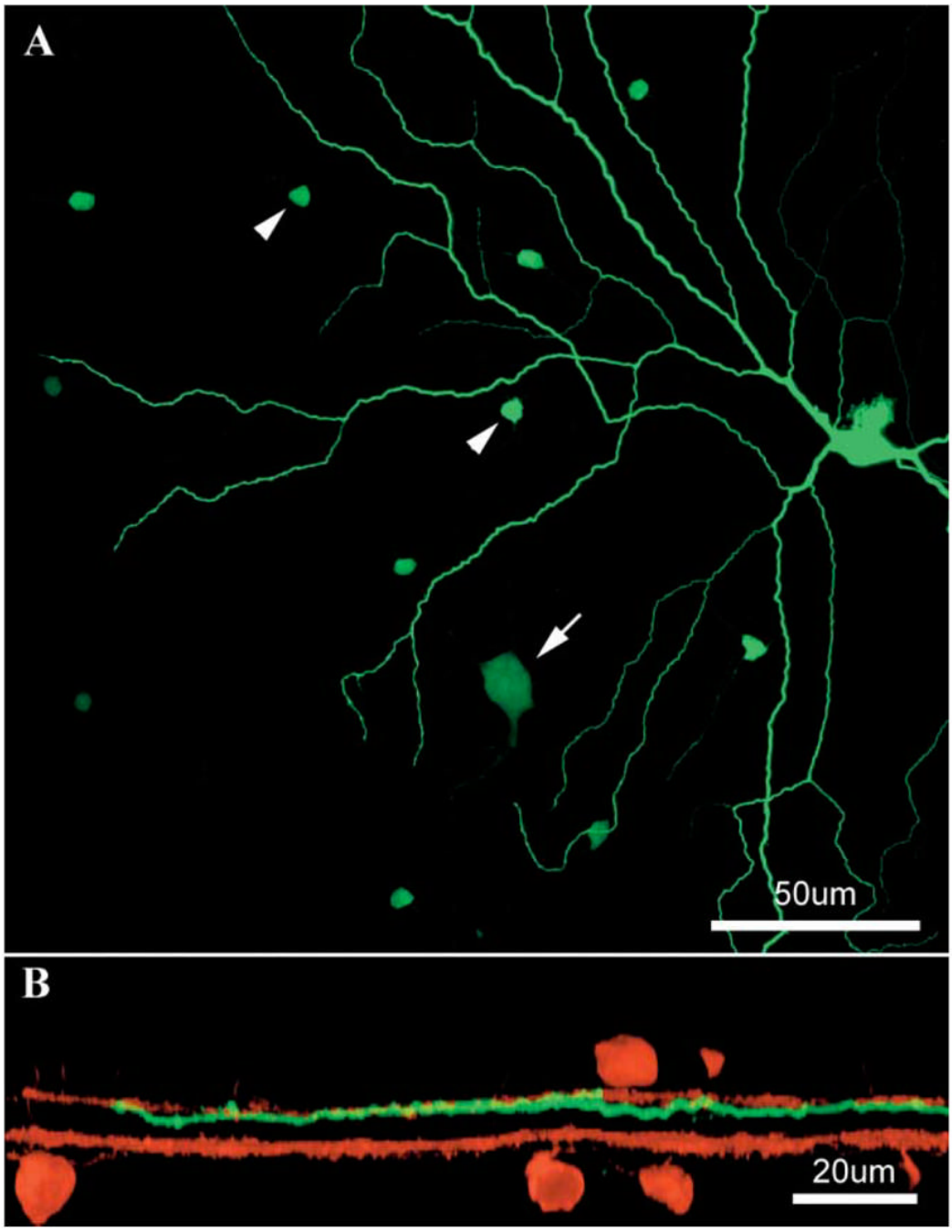


**Fig. 5.**

Double-label confocal images of an OFF α ganglion cell. A: Wholemount view shows part of the dendritic field of a Neurobiotin injected OFF α cell (green). The injected soma is marked by some dye leakage. This ganglion cell type is typically dye coupled to amacrine cells (arrowheads) and other OFF α cells (arrow). B: *Z*-axis reconstruction shows that the OFF α ganglion cells is stratified just below cholinergic *a* in the IPL. The cholinergic strata are labeled red.

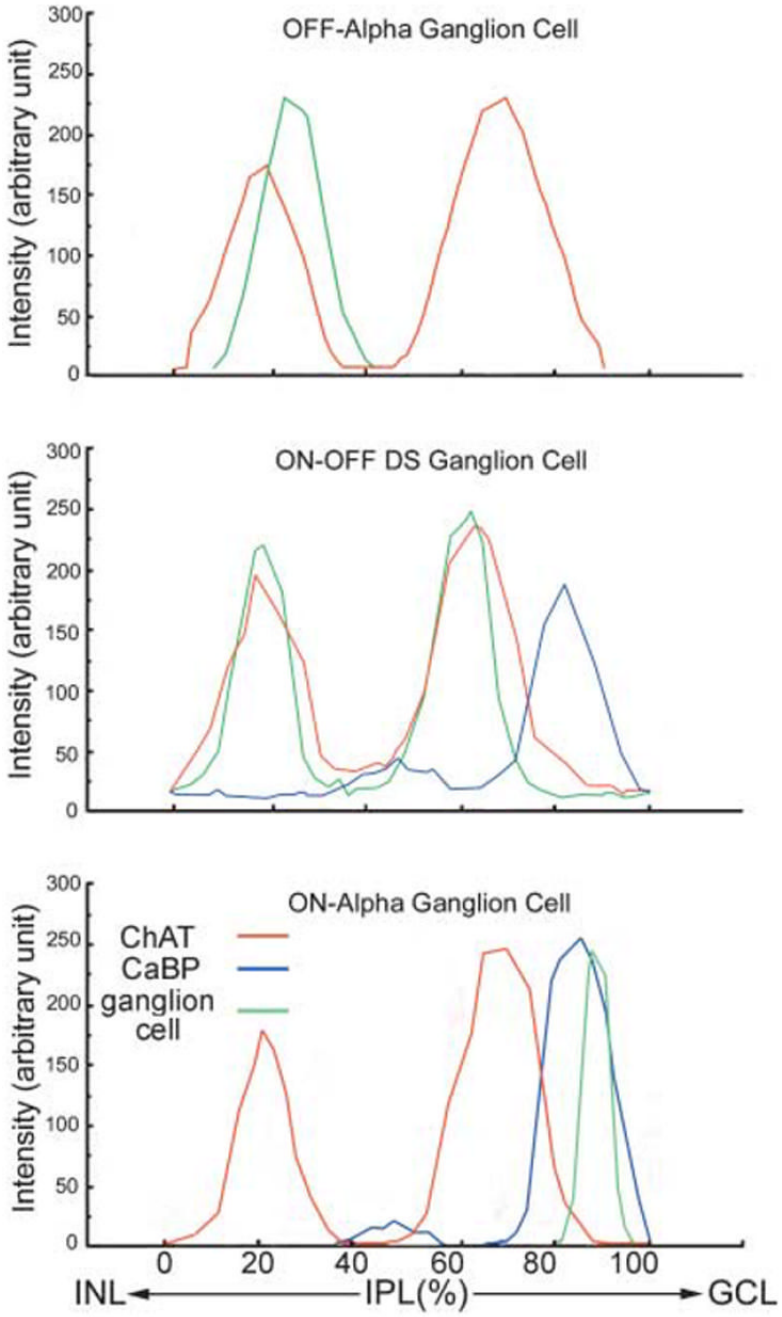


**Fig. 6.**

Density profiles across the IPL. Labeling for choline acetyltransferase is shown in red. There are two prominent bands at approximately 20 and 70 % depth in the IPL (Famiglietti & Tumosa, 1987). Cabindin labeling is shown in blue. There is a major peak, distinctly below cholinergic *b*, corresponding to the terminals of calbindin cone bipolar terminals (Massey & Mills, 1996), and a minor peak at approximately the middle of the IPL, contributed by some calbindin positive wide-field amacrine cells. *Top*: Density profile for an OFF α ganglion cell (green) shows a peak just below the upper cholinergic band. *Middle*: Density profile for an ON/OFF DS ganglion cell shows two peaks, coincident with the cholinergic bands. *Bottom*: Density

profile for an ON α ganglion cell shows a peak just below the lower cholinergic band, overlapping with the peak due to the calbindin bipolar terminals.

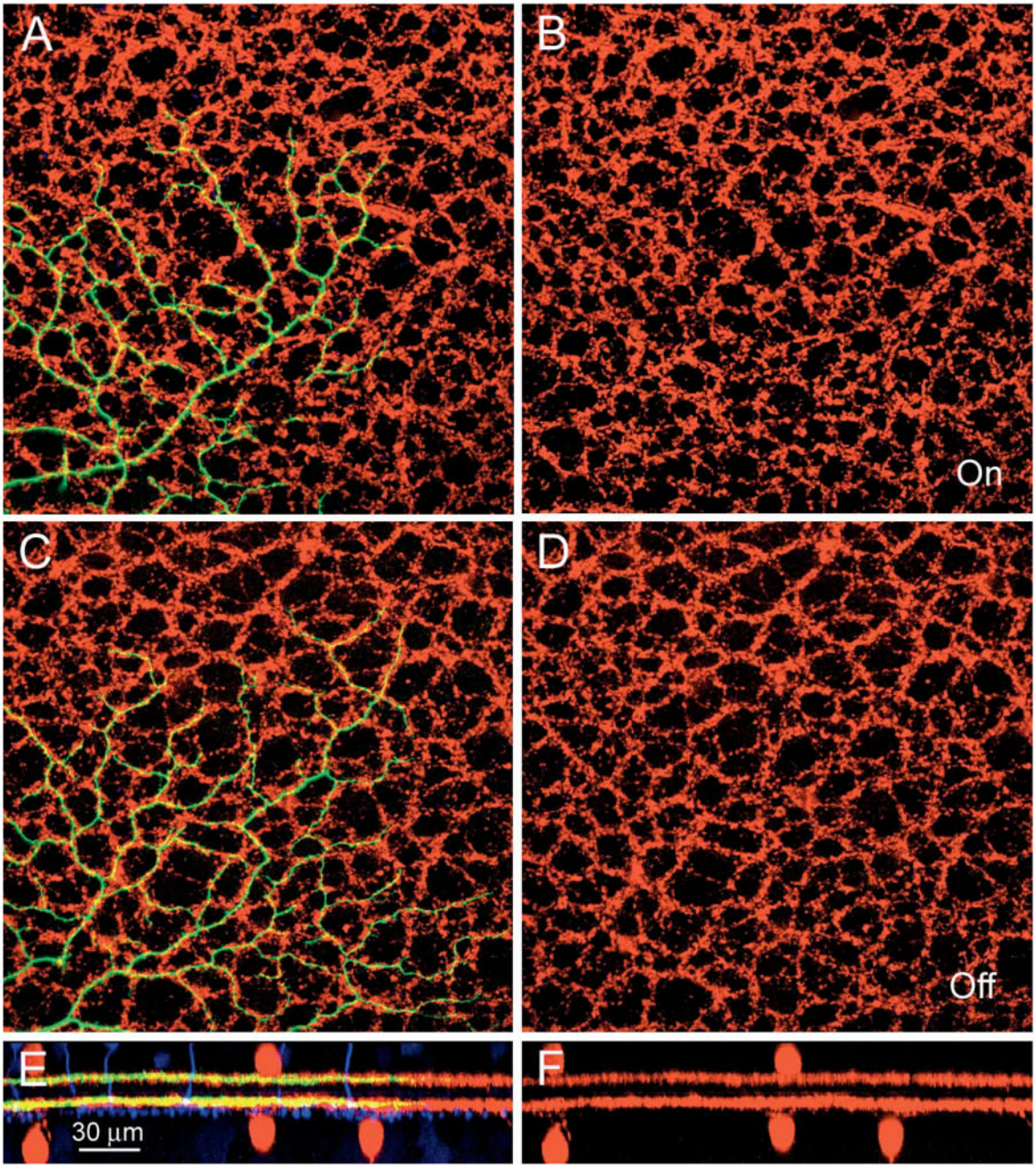


**Fig. 7.**

Cofasiculation with the cholinergic matrices. A: Wholemount shows the OFF dendritic field of an ON/OFF DS ganglion cell (green) which runs in the matrix of cholinergic *a* (red). B: The matrix of cholinergic *a* alone (red). C: Wholemount view showing the ON dendrites (green) cofasciculating with the lower cholinergic plexus (red). D: The ON cholinergic matrix alone. E: *Z*-axis reconstruction shows the bistratified ON/OFF DS cell (green) stratified at exactly the same level as the cholinergic bands (red). The terminals of calbindin bipolar cells (blue) ramify just below cholinergic b. F: *Z*-axis reconstruction of the cholinergic amacrine cells alone (red).

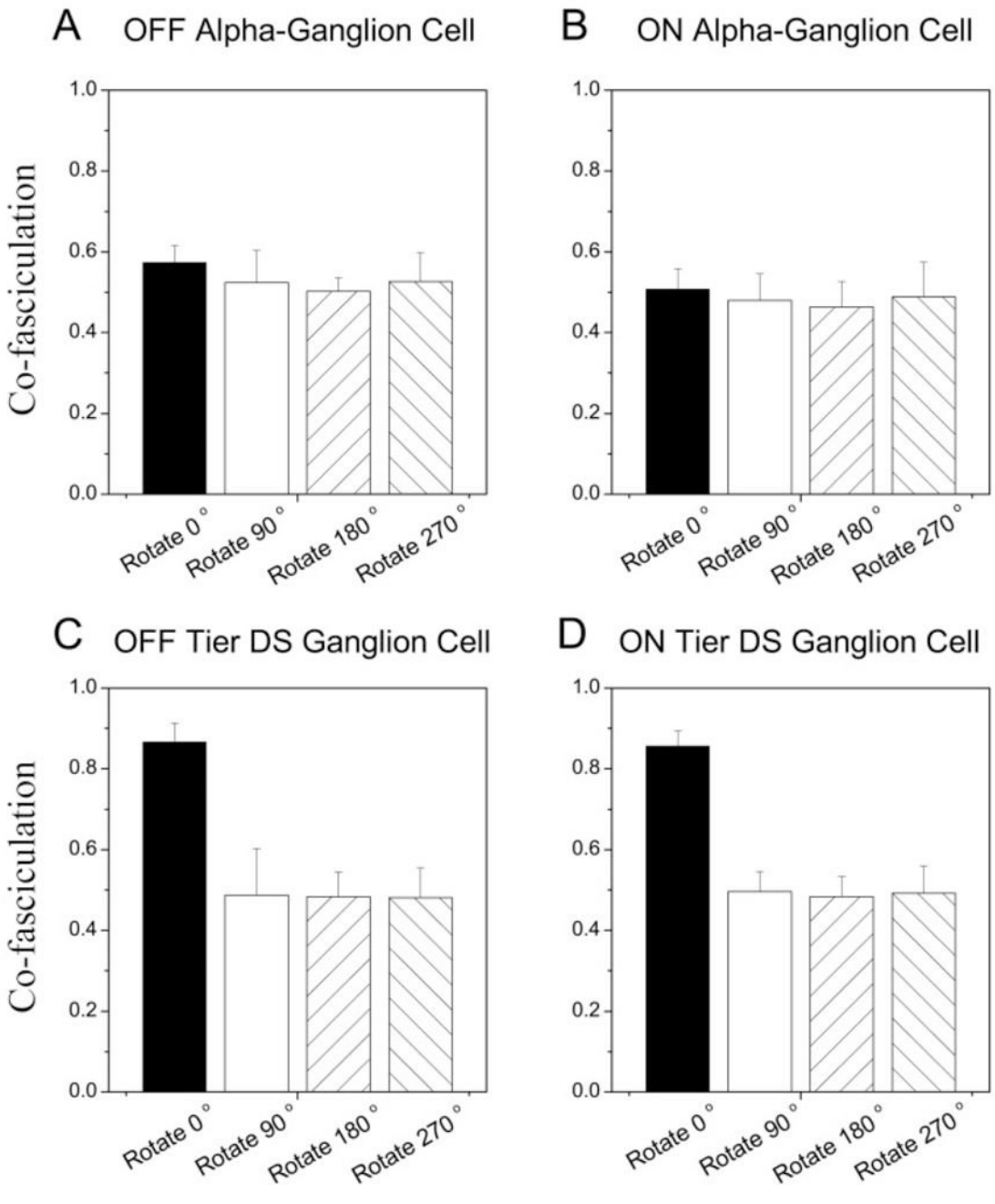


**Fig. 8.**

Statistical analysis of co-fasciculation with the cholinergic matrix. The co-fasciculation between the two sets of processes was measured in the original confocal image for comparison with images were one label was rotated by 90 deg, 180 deg, or 270 deg to estimate the number of overlapping pixels expected by chance. Only co-fasciculation between the dendrites of ON/OFF DS cells and the cholinergic matrix occurred more frequently than expected due to chance. Thus, the original orientation was the same height for A, OFF α ganglion cells and B, ON α ganglion cells. In contrast, the peak height for both OFF (C) and ON (D) strata for ON/OFF DS ganglion cells was approximately twice as high as the controls. This is the signature of co-fasciculation as opposed to chance overlap.

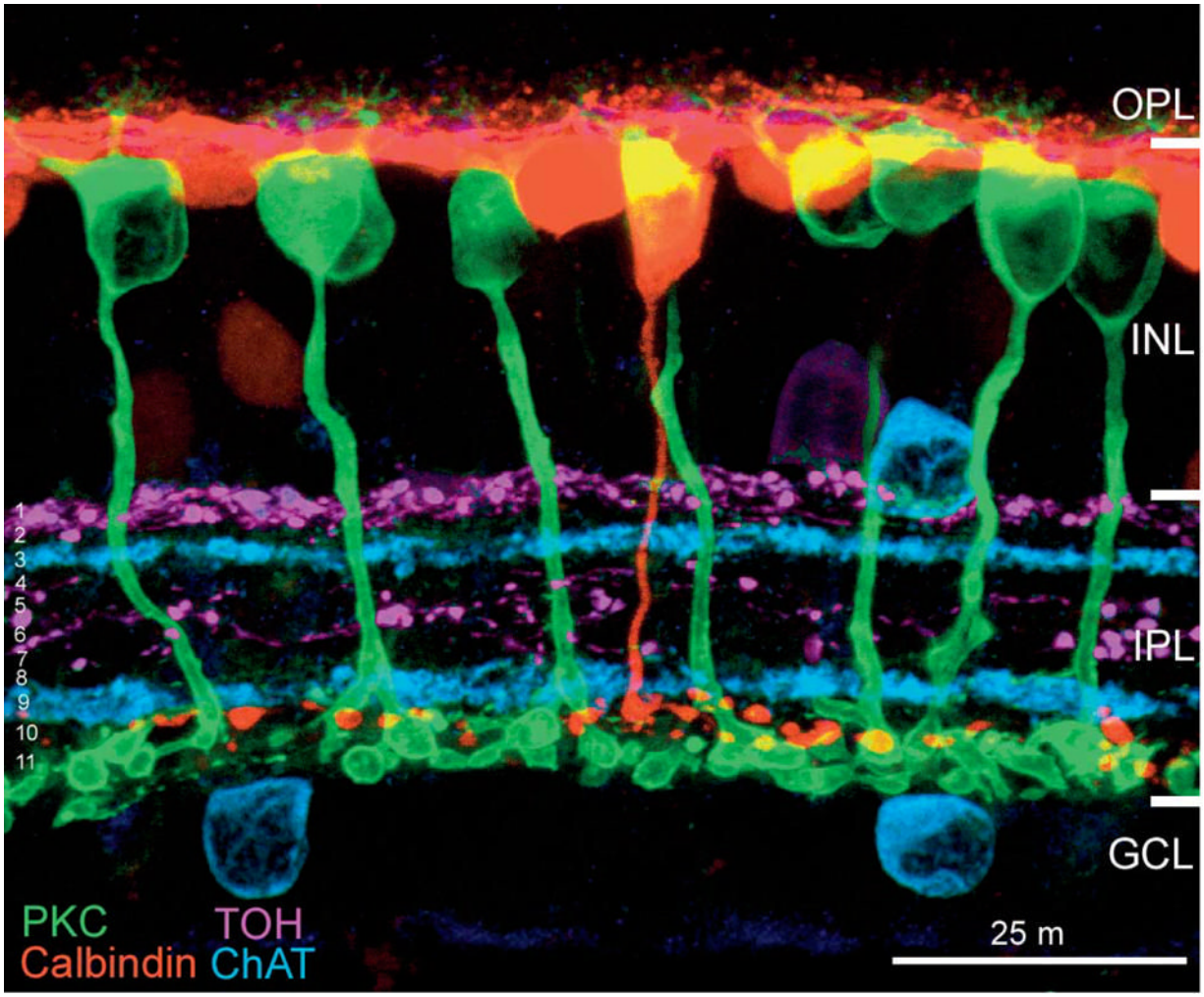


**Fig. 9.**

Quadruple labeling of the IPL. An antibody to PKC was used to label rod bipolar cells (green). Rod bipolar cells send their axons through the IPL and their terminals ramify at the lowest level of the IPL. An antibody to choline acetyltransfrease was used to label cholinergic amacrine cells (light blue). Dopaminergic amacrine cells at the upper margin of the IPL were labeled with an antibody against TOH. An antibody against calbindin (red) labeled horizontal cells at the top of the INL and calbindin bipolar cells, one of which is in the center of the field. Calbindin bipolar cells have somas in the INL and axons which descend to form a band of terminal just below the lower cholinergic band. At least 11 different layers may be separated in this image (see text). This sets a lower limit on the number of layers in the IPL.